Chemistry A European Journal

Chemistry Europe
European Chemical Societies Publishing

Cover Feature:
H. Dong and co-workers
Modular Design and Self-assembly of pH-Responsive Multidomain Peptides Incorporating Non-natural Ionic Amino Acids

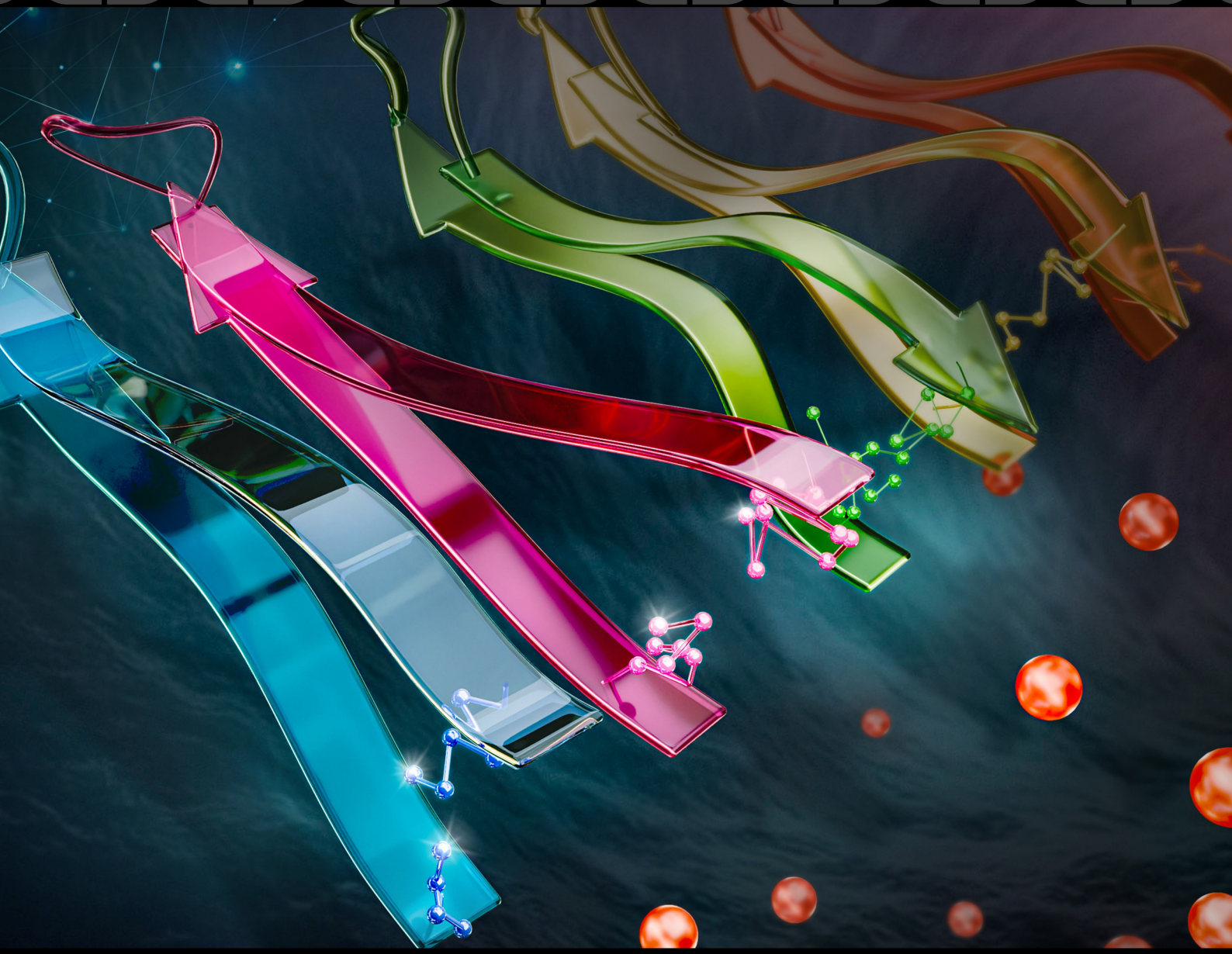

WILEY VCH

67/2024

Chemistry–A European Journal
Research Article
doi.org/10.1002/chem.202403085
Chemistry Europe
European Chemical Societies Publishing
www.chemeurj.org

Modular Design and Self-assembly of pH-Responsive Multidomain Peptides Incorporating Non-natural Ionic Amino Acids

Haritha Asokan-Sheeja,[a] Debdatta Das,[a] Jenny N. Nguyen,[a] Na Nguyen,[b] Tran Van Khanh Pham,[b] Kytai T. Nguyen,[b] and He Dong*[a]

Stimuli-responsive peptides, particularly pH-responsive variants, hold significant promise in biomedical and technological applications by leveraging the broad pH spectrum inherent to biological environments. However, the limited number of natural pH-responsive amino acids within biologically relevant pH ranges presents challenges for designing rational pH-responsive peptide assemblies. In our study, we introduce a novel approach by incorporating a library of non-natural amino acids featuring chemically diverse tertiary amine side chains. Hydrophobic and ionic properties of these non-natural amino acids facilitate their incorporation into the assembly domain when uncharged, and electrostatic repulsion promotes disassembly under lower pH conditions. Furthermore, we observed a direct relationship between the number of substitutions and the hydrophobicity of these amino acids, influencing their pH-responsive properties and enabling rational design based on desired transitional pH ranges. The structure-activity relationship of these pH-responsive peptides was evaluated by assessing their antimicrobial properties, as their antimicrobial activity is triggered by the disassembly of peptides to release active monomers. This approach not only enhances the specificity and controllability of pH responsiveness but also broadens the scope of peptide materials in biomedical and technological applications.

Stimuli-responsive peptide self-assembly are becoming increasingly popular in numerous applications such as drug delivery, targeted therapy, and tissue engineering.[1] They possess the remarkable ability to self-assemble into smart materials that detect environmental changes and undergo specific morphological transformations. Recently, there has been increased interests in advancing these stimuli-responsive self-assembled peptides, with pH-responsive variants receiving significant attention for their utilization of natural pH fluctuations within the body.[2] Unlike other peptide-based drug delivery systems, which often struggle with target specificity, pH-responsive peptides could potentially enhance clinical outcomes. These pH-responsive peptides can be engineered to leverage pH variations across different bodily environments, spanning organ, tissue, and cellular levels.[3] By harnessing these pH gradients, pH-based drug delivery systems can efficiently deliver therapeutic agents to specific tissues or even cellular compartments.

Among the limited variety of naturally occurring amino acids, those that are pH-responsive are particularly scarce. Many of these amino acids have an intrinsic pK_a which is highly acidic or basic, therefore limiting their utility for biological applications. Histidine is the only natural amino acid that has a transition pH within physiologically relevant pH range and has been commonly used for the synthesis of pH-responsive peptide assemblies. To explore and expand the pH-responsive chemistry in peptide self-assembly, our group recently introduced a novel approach to develop pH-responsive peptides using non-natural amino acids bearing tertiary butylamine and tertiary propylamine groups.[4] These amino acids were integrated into the hydrophobic core of peptide assemblies due to their hydrophobic nature when deprotonated, owing to the presence of the alkyl chain. Upon lowering the pH, the tertiary amines within the hydrophobic core become protonated, leading to electrostatic repulsion that promotes disassembly. Interestingly, within the locally hydrophobic microenvironment created by self-assembly, these tertiary amine side groups exhibit a lower pK_a in the weakly acidic to neutral pH range, contrary to their typical basic pK_a in isolation. The current study aims to expand the repertoire of non-natural amino acids for diverse biomedical applications by developing a library of pH-responsive peptides. This library demonstrates pH responsiveness within specific pH ranges, from weakly acidic to neutral pH, allowing for the selection of peptide designs tailored to the pH conditions of the target site.

The multidomain peptides (MDPs) used in this study are summarized in Table 1 detailing their primary sequences. The control peptide, QL, features the sequence $K_4G_5(QW)(QL)_5$, composed of six repeating units of an alternating hydrophilic-hydrophobic motif $(QW)(QL)_5$ (Q: glutamine, L: leucine, W: tryptophan; 5 denotes the number of QL repeats). Tryptophan serves as a UV-Vis reporter to ensure precise concentration determination. Previous findings indicate that these polar-nonpolar units drive the formation of sandwich-like nanofibers,

[a] H. Asokan-Sheeja, D. Das, J. N. Nguyen, H. Dong
Department of Chemistry and Biochemistry, The University of Texas at Arlington, 701 S Nedderman Dr, Arlington, 76019 TX, USA
E-mail: he.dong@uta.edu
[b] N. Nguyen, T. V. K. Pham, K. T. Nguyen
Department of Bioengineering, The University of Texas at Arlington, 701 S Nedderman Dr, Arlington, 76019 TX, USA

Supporting information for this article is available on the WWW under https://doi.org/10.1002/chem.202403085

Table 1. MDP sequences used in this study.

Name	N-	Sequence	C-
QL	CH_3CO	KKKKGGGGGQWQLQLQLQLQL	$CONH_2$
$3X_p$	CH_3CO	KKKKGGGGGQWQLQX$_p$QX$_p$QX$_p$QL	$CONH_2$
$2X_p$	CH_3CO	KKKKGGGGGQWQLQX$_p$QLQX$_p$QL	$CONH_2$
$3X_b$	CH_3CO	KKKKGGGGGQWQLQX$_b$QX$_b$QX$_b$QL	$CONH_2$
$2X_b$	CH_3CO	KKKKGGGGGQWQLQX$_b$QLQX$_b$QL	$CONH_2$
$3X_{ch}$	CH_3CO	KKKKGGGGGQWQLQX$_{ch}$QX$_{ch}$QX$_{ch}$QL	$CONH_2$
$2X_{ch}$	CH_3CO	KKKKGGGGGQWQLQX$_{ch}$QLQX$_{ch}$QL	$CONH_2$

where leucine and tryptophan are embedded within the hydrophobic core of the assembly.[5]

To introduce pH-responsiveness to the MDPs, leucine residues in the sequence were substituted with a synthetic non-natural amino acid denoted as X, featuring a dialkylamino methyl group on its side chain. Our previous work demonstrates that these self-assembling MDPs form sandwich-like nanofibers where the non-natural amino acids occupy the hydrophobic domain of the peptide. The presence of non-natural amino acids induces an ionization-dependent self-assembly process. Upon assembly, the hydrophobic pocket stabilizes the neutral form of X, thereby significantly lowering the pK_a of the tertiary amine group on X to a nearly neutral or weakly acidic range. The pH-dependent self-assembly of these MDPs is influenced by two main factors. First, the hydrophobic nature of the non-natural amino acids promotes self-assembly by minimizing unfavorable interactions with the hydrophilic environment. Second, ionization of the tertiary amine leads to charge-charge repulsions within the hydrophobic core, potentially causing disassembly of the structure. Our hypothesis is the transition pH of the MDPs is controlled by the balance between the hydrophobic and charge-charge interactions. We tested this hypothesis with six MDP variants consisting of X residue with different hydrophobicity and substitution degrees. More importantly we aim to develop peptide assemblies that exhibit highly tunable pH-responsiveness in the biological relevant pH range, making them suitable for a wide array of biological applications.

The synthetic route for all the Fmoc-protected amino acids, i.e. Fmoc-X_p, Fmoc-X_b, and Fmoc-X_{ch} was described in Figure S1.[4] The synthesis was confirmed by NMR spectroscopy and ESI mass spectrometry (Figure S2–4). The Fmoc-protected amino acids can be readily incorporated at specific sites of MDPs through solid-phase peptide synthesis. Figure 1a depicts the primary structure of the MDP with double and triple substitutions, denoted as 2X and 3X. Figure 1b illustrates the pH-dependent assembly/disassembly process with the assembled state defined as "OFF" and the disassembly as "ON". Peptide synthesis was confirmed by mass spectrometry (Figure S5a–n). As demonstrated in our prior research, non-natural amino acids are strategically incorporated into the sequence to reside within the hydrophobic core of the self-assembly when uncharged. However, under lower pH conditions, the tertiary amines become protonated. Due to the proximity of these

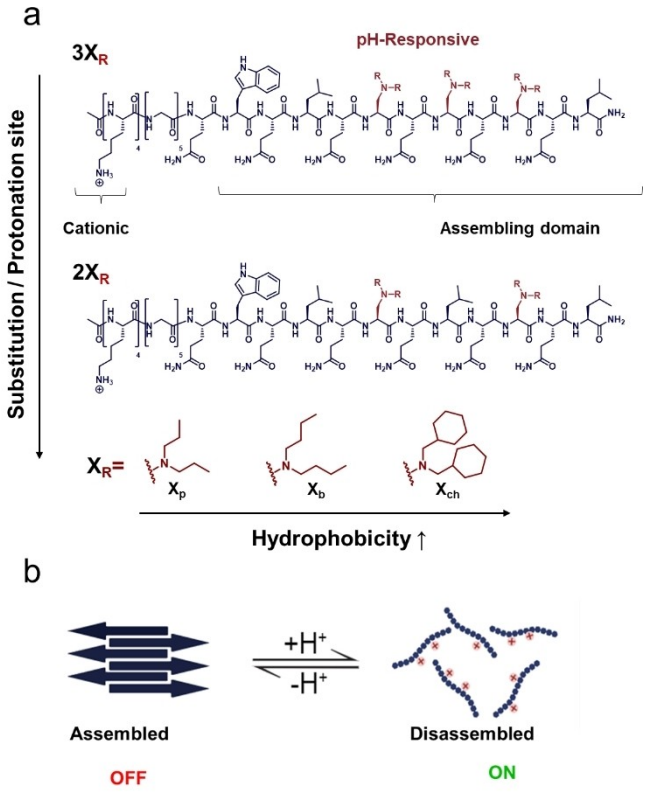

Figure 1. a) Chemical structure of peptides $3X_R$ and $2X_R$. The peptide design contains an assembling domain featuring repetitive hydrophobic-hydrophilic subunits. Hydrophobic ionizable amino acids are introduced to induce pH-responsiveness. The numbers 3 and 2 in the peptide denote the number of pH-responsive amino acid groups. **b**) Schematic representation of peptide assembly at basic conditions and disassembly, defined as the "OFF" state and disassembly when the ionic amino acids are protonated at acidic conditions defined as the "ON" state.

charged amines within the self-assembly, electrostatic repulsion triggers disassembly. Protonation of X residues is a critical step in triggering disassembly, and it highly depends on the local hydrophobic environment. Our current study aims to study the effect of the role of hydrophobicity as well as the number of protonation sites in controlling the pH-dependent disassembly.

Fluorescence studies using NBD (nitrobenzodiazole)-labelled peptides were first conducted to investigate the pH-dependent transitions. Changes in fluorescence intensity were monitored across different pH values (Figure S7). Upon self-assembly, the NBD fluorescence decreased due to fluorescence quenching. Monitoring the decrease in intensity served as a tool to determine the transition pH. The normalized fluorescence intensity was determined using the formula $\frac{I-Imin}{Imax-Imin}$ where I represents the fluorescence intensity at a specific pH value, and I_{max} and I_{min} denote the maximum and minimum fluorescence intensities observed in the ON and OFF states, respectively. The normalized fluorescence intensity values were subsequently plotted as a function of pH to quantitatively evaluate the pH-responsive characteristics of the peptide (Figure 2a). The data points were fitted to a logistic curve, and the midpoint of the curve was identified as the transition pH, as presented in Table S1. As anticipated, the side chain characteristics of the

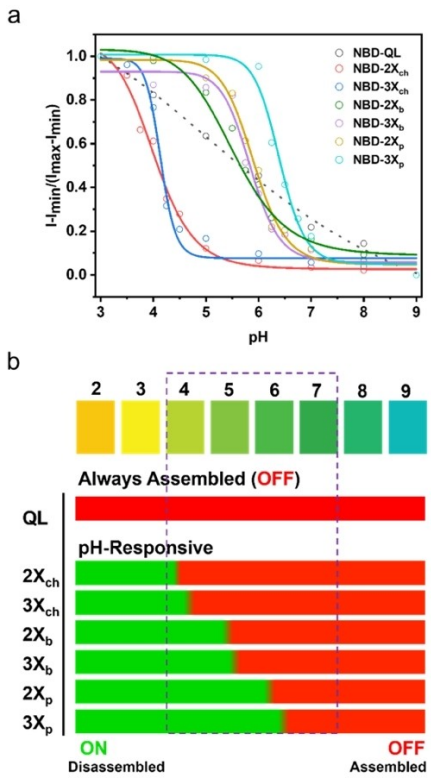

Figure 2. a) Normalized fluorescence emission intensity at λmax plotted against pH for NBD-labelled peptide. The fluorescence intensity decreases upon assembly due to fluorescence quenching. b) Illustration showing the pH-responsive window of peptides.

amino acids significantly influence the transition pH of the peptide. Peptides containing more hydrophobic amino acids require more acidic conditions for protonation compared to peptides with less hydrophobic residues. This phenomenon likely results from the integration of hydrophobic side chains within the peptide assembly. The increased hydrophobic interactions facilitate self-assembly, and disassembly is achieved only when the H^+ concentration reaches a sufficiently high level to disfavor assembly. As the number of amino acid substitutions increased, the transition pH value shifted to higher levels. This shift is attributed to the increased number of protonation sites, which, upon protonation, promote disassembly. These findings are illustrated in Figure 2b. The QL peptide, which is non-responsive, consistently remains in the assembled or the 'OFF' state. In contrast, pH-responsive peptides can exist in either the 'ON' (disassembled) or 'OFF' (assembled) state depending on the pH. This structural transition is contingent upon their transition pH; above the transition pH, the peptides remain in the 'OFF' state, whereas below the transition pH, they transition to the 'ON' state.

Thioflavin T (ThT), a small molecule known for enhanced fluorescence upon binding to β-sheet amyloid, was used for estimating the transition pH of all peptides.[6] The fluorescence emission spectra of the pH-responsive peptides exhibited increased intensity due to the formation of amyloid-like β-sheet secondary structures in their assembled state (OFF). This elevated fluorescence is attributed to the structural transformation that enhances Thioflavin T (ThT) fluorescence upon binding to β-sheets. Conversely, upon disassembly of the peptides (ON), a decrease in ThT fluorescence intensity was observed. Notably, for 3X$_{ch}$ and 2X$_{ch}$ peptides, there were no significant changes in fluorescence intensity of ThT across the entire pH range. While higher resolution microscopic or spectroscopic analysis is needed, the two peptides may have a different packing order within the fiber compared to the antiparallel arrangement adopted in canonical amyloid-like β-sheet nanofibers. The determination of transition pH, based on plotting the fluorescence emission intensity of Thioflavin T (ThT) at λ_{max} 480 nm, displayed a trend consistent with that observed for the NBD-labeled peptide (Figure S8 and Table S1). However, this method proved less informative when the assembled structures deviated from the canonical amyloid-like β-sheet secondary structure.

Circular dichroism (CD) spectroscopy was further employed to determine the transition pH of the peptides showing a pH-dependent structural transition from self-assembled β-sheets to random coils (Figure 3a–f). The molar ellipticity at 200 nm was plotted against pH to identify the transition pH (Figure 3g). Transition pH values were calculated by fitting the CD data to a logistic curve, and these values are listed in Table S1. As anticipated, the transition pH decreased with increasing hydrophobicity of the side chains. Moreover, the transition pH decreased with reduced substitution. Based on the CD spectroscopy results, the peptides followed the order of transition pH: 3X$_p$ > 2X$_p$ > 3X$_b$ > 2X$_b$ > 3X$_{ch}$ > 2X$_{ch}$. This is consistent with NBD-based fluorescence assay. Further TEM analysis confirmed that the peptides assembled into elongated nanofibers at pH 7.4. 3X$_p$ exhibited reduced nanofiber formation at pH 7.4 due to its transition pH in proximity to physiological pH, whereas all other peptides formed extensive nanofibers (Figure 4). Notably, X$_{ch}$-containing peptides appeared to form worm-like fibers rather

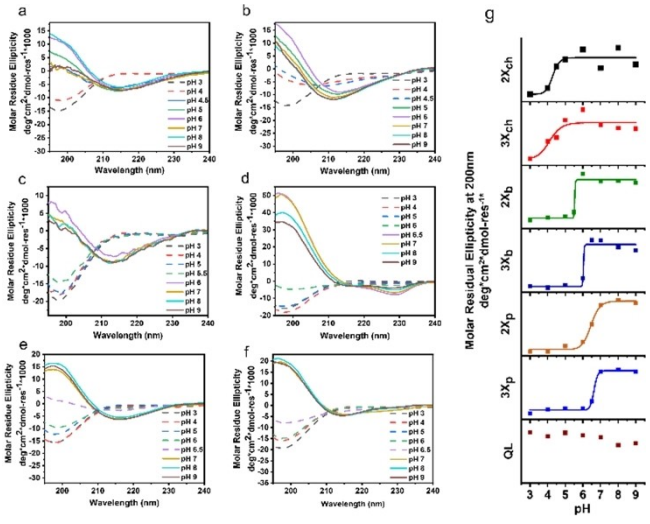

Figure 3. a–f) pH-dependent CD spectra of peptides with non-natural amino acid substitutions. **g)** Molar residual ellipticity at 200 nm of 3X$_b$ and 2X$_b$ from CD spectroscopy measurement plotted against pH. The negative value of ellipticity indicates the presence of monomeric structures. As the pH increases, the peptide starts to assemble, as indicated by the positive ellipticity value. Peptide concentration: 50 μM in BR buffer.

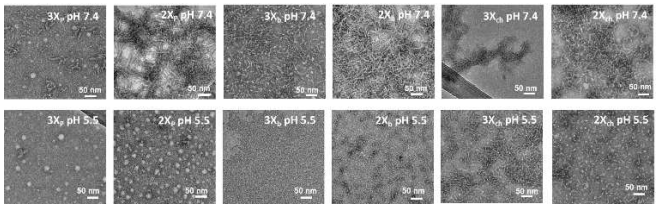

Figure 4. TEM of peptides showing different morpholgy at pH 5.5 and 7.4. The peptide solutions were prepared at 100 μM in BR buffer.

than amyloid-mimetic structures. TEM analysis at pH 5.5 evaluated the acid-triggered disassembly of the peptides. As anticipated, peptides with a transition pH above 5.5 exhibited reduced or absent fiber content at this pH. However, $3X_{ch}$ and $2X_{ch}$ peptides displayed nanofiber formation at pH 5.5 due to their lower transition pH values, which are below 5.5.

To explore the structure-activity relationship of these peptides at specific pHs, we evaluated their pH-dependent antimicrobial activity. As previously demonstrated, the alternating hydrophobic-hydrophilic (QL) domain enables leucine residues to form local hydrophobic clusters, while external lysine residues aggregate into cationic clusters to target and disrupt bacterial lipid membranes. In their assembled state, hydrophobic residues are shielded within the assembly and cannot interact effectively with bacterial membranes, rendering the peptides inactive. Antimicrobial activity is only triggered upon disassembly, which releases the active monomeric peptides which allow the exposure and insertion of the hydrophobic residues into the lipid membrane. Thus, the antimicrobial effectiveness of the peptide is closely tied to its transition pH. To advance the development of responsive antimicrobial materials, we evaluated the peptides' antimicrobial activity against gram-negative bacterium *P. aeruginosa* using the standard minimum inhibitory concentration (MIC) assay (Table 2). At pH 7.4, all peptides adopt an assembled structure, resulting in a lack of antimicrobial activity with MIC values above 160 μM. At pH 5.5 which is below the transition pH of $3X_p$, $2X_p$, $3X_b$ and $2X_b$, the peptides are disassembled showing acid-induced antimicrobial activity with MIC values at 20 μM. At pH 5.5, $2X_{ch}$ and $3X_{ch}$ and QL remain assembled with a transition pH below the testing pH and therefore being inactive against *P. aeruginosa*. To further study the physical interaction between the peptide and the bacteria, membrane localization assay was carried out using NBD-labelled peptides (Figure 5a). Three peptides were selected for the test, including the control QL peptide, $2X_b$ with transition pH at 5.73, and $2X_{ch}$ with a transition pH at 4.02 based on the NBD fluorescence measurement. The bacteria were incubated with NBD-labeled peptides at pH 7.4 and 5.5. We observed an increased binding for NBD-$2X_b$ at pH 5.5 indicating disassembly of peptide and binding of the monomeric peptides to the bacterial membrane. $2X_{ch}$ and QL have much lower membrane binding capability as demonstrated by the minimal fluorescence intensity at both neutral and acidic pH conditions, suggesting the lack of pH-responsiveness under the acidic condition. Figure 5b illustrates the effect of pH-dependent structural transitions of peptides on their functional activity, particularly enhanced binding. In the OFF state, the peptides aggregate into larger structures, which inhibit interaction with the bacterial membrane because the hydrophobic residues are buried within the assembly. As a result, these residues are not available to interact with the lipid membrane. However, upon transitioning to the ON state at a lower pH, the peptides disassemble, exposing the hydrophobic domains. This exposure facilitates binding to the bacterial membrane and enhances the peptides' ability to promote acidity-triggered bacterial killing.

In conclusion, we showed the design and synthesis of pH-responsive self-assembling peptides incorporating hydrophobic ionizable amino acids, allowing for adjustable transition pH suited for diverse biological applications. The impact of non-natural amino acid and substitution number was investigated, strategically placing ionizable residues within a *de novo* designed MDP. These residues are encapsulated within the hydrophobic core of sandwich-like nanofibers formed by the MDP. Increasing the hydrophobicity of non-natural amino acid side chains lowered the transition pH required for peptide assembly, necessitating a more acidic environment for disassembly initiation. Moreover, varying the number of protonation sites through amino acid substitutions influenced the disassem-

Table 2. MIC results of MDPs against *P. aeruginosa.*

Peptide	pH 7.4	pH 5.5
QL	>160 μM	>160 μM
$3X_p$	>160 μM	20 μM
$2X_p$	>160 μM	20 μM
$3X_b$	>160 μM	20 μM
$2X_b$	>160 μM	20 μM
$3X_{ch}$	>160 μM	>160 μM
$2X_{ch}$	>160 μM	>160 μM

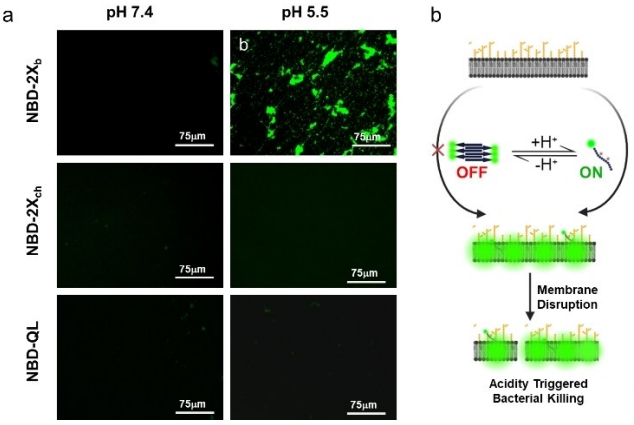

Figure 5. a) Membrane localization assay of NBD-labelled peptide against *P. aeruginosa.* Top panel: *P. aeruginosa* treated with NBD-$2X_b$ at pH 7.4, and pH 5.5. middle panel: *P. aeruginosa* treated with NBD-$2X_{ch}$ at pH 7.4, and pH 5.5. Bottom panel: *P. aeruginosa* treated with NBD-QL at pH 7.4, and pH 5.5. Peptide concentration 40 μM in Tris (20 mM, pH 7.4) or MES (20 mM, pH 5.5). **b**) Schematic representation of acidity triggered membrane binding and bacterial killing of peptides.

bly process, with more sites facilitating lower transition pH values. Although we showed the proof-of-concept design in pH-responsive MDP self-assembly, these non-natural ionic amino acids can be readily incorporated in many other peptide assemblies where hydrophobic effects drive the assembly process. The strategy will open a new route to construct pH-responsive peptide materials with highly tunable transition pH for various biological applications with different pH gradient demands.

Acknowledgements

This study was supported by the National Science Foundation (DMR 1341925), the start-up funds from the University of Texas at Arlington and the National Science Foundation Partnership for Research and Education in Functional Materials under the award # DMR 2425164.

Conflict of Interests

The authors declare no conflict of interest.

Data Availability Statement

Research data are not shared

Keywords: Peptide self-assembly · pH-responsive · Non-natural amino acids · Antimicrobial

[1] a) C. J. Bowerman, B. L. Nilsson, *J. Am. Chem. Soc.* **2010**, *132*, 9526–9527; b) W. Chen, S. Li, J. C. Lang, Y. Chang, Z. Pan, P. Kroll, X. Sun, L. Tang, H. Dong, *Small* **2020**, *16*, 2002780; c) Y. Ding, D. Zheng, L. Xie, X. Zhang, Z. Zhang, L. Wang, Z. W. Hu, Z. Yang, *J. Am. Chem. Soc.* **2023**, *145*, 4366–4371; d) D. Gupta, V. Gupta, D. Nath, C. Miglani, D. Mandal, A. Pal, *ACS Appl. Mater. Interfaces* **2022**, *15*, 25110–25121; e) Y. Li, C. A. Foss, D. D. Summerfield, J. J. Doyle, C. M. Torok, H. C. Dietz, M. G. Pomper, S. M. Yu, *Proc. Natl. Acad. Sci.* **2012**, *109*, 14767–14772; f) Y. Liu, Y. Yang, C. Wang, X. Zhao, *Nanoscale* **2013**, *5*, 6413–6421; g) R. J. Mart, R. D. Osborne, M. M. Stevens, R. V. Ulijn, *Soft Matter.* **2006**, *2*, 822–835; h) R. Mu, D. Zhu, S. Abdulmalik, S. Wijekoon, G. Wei, S. G. Kumbar, *Bioact. Mater.* **2024**, *35*, 181–207; i) A. Shah, M. S. Malik, G. S. Khan, E. Nosheen, F. J. Iftikhar, F. A. Khan, S. S. Shukla, M. S. Akhter, H. B. Kraatz, T. M. Aminabhavi, *Chem. Eng. J.* **2018**, *353*, 559–583; j) S. Sun, H. W. Liang, H. Wang, Q. Zou, *ACS Nano* **2022**, *16*, 18978–18989; k) W. Tan, Q. Zhang, M. C. Quiñones-Frías, A. Y. Hsu, Y. Zhang, A. Rodal, P. Hong, H. R. Luo, B. Xu, *J. Am. Chem. Soc.* **2022**, *144*, 6709–6713; l) S. Yang, Y. Chang, S. Hazoor, C. Brautigam, F. W. Foss Jr, Z. Pan, H. Dong, *ChemBioChem* **2021**, *22*, 3164–3168; m) S. Yang, D. Xu, H. Dong, *J. Mater. Chem. B* **2018**, *6*, 7179–7184; n) Y. Zhou, Q. Li, Y. Wu, X. Li, Y. Zhou, Z. Wang, H. Liang, F. Ding, S. Hong, N. F. Steinmetz, *ACS Nano* **2023**, *17*, 8004–8025.

[2] a) Z. Li, Y. Zhu, J. B. Matson, *ACS Appl. Bio Mater.* **2022**, *5*, 4635–4651; b) W. Chen, S. Hazoor, R. Madigan, A. A. Adones, U. K. Chintapula, K. T. Nguyen, L. Tang, F. W. Foss Jr, H. Dong, *Mater. Today Adv.* **2022**, *16*, 100288; c) S. H. Nam, J. Jang, D. H. Cheon, S. E. Chong, J. H. Ahn, S. Hyun, J. Yu, Y. Lee, *J. Controlled Release* **2021**, *330*, 898–906; d) A. S. Carlini, W. Choi, N. C. McCallum, N. C. Gianneschi, *Adv. Funct. Mater.* **2021**, *31*, 2007733; e) W. Chen, S. Li, P. Renick, S. Yang, N. Pandy, C. Boutte, K. T. Nguyen, L. Tang, H. Dong, *J. Mater. Chem. B* **2019**, *7*, 2915–2919; f) M. Gontsarik, A. Yaghmur, Q. Ren, K. Maniura-Weber, S. Salentinig, *ACS Appl. Mater. Interfaces* **2018**, *11*, 2821–2829; g) X. R. Zhou, R. Ge, S. Z. Luo, *J. Pept. Sci.* **2013**, *19*, 737–744; h) J. N. Shera, X. S. Sun, *Biomacromolecules* **2009**, *10*, 2446–2450; i) A. Aggeli, M. Bell, L. M. Carrick, C. W. Fishwick, R. Harding, P. J. Mawer, S. E. Radford, A. E. Strong, N. Boden, *J. Am. Chem. Soc.* **2003**, *125*, 9619–9628; j) X. Li, M. Fu, J. Wu, C. Zhang, X. Deng, A. Dhinakar, W. Huang, H. Qian, L. Ge, *Acta Biomater.* **2017**, *51*, 294–303.

[3] a) W. Li, Q. Bie, K. Zhang, F. Linli, W. Yang, X. Chen, P. Chen, Q. Qi, *Food Chem. X* **2024**, 23, 101645;b) D. Wang, Z. Fan, X. Zhang, H. Li, Y. Sun, M. Cao, G. Wei, J. Wang, *Langmuir* **2020**, *37*, 339–347; c) J. Zhang, W. Lin, L. Yang, A. Zhang, Y. Zhang, J. Liu, J. Liu, *Biomater. Sci.* **2022**, *10*, 854–862; d) Z. Wang, J. Zhang, Y. Wang, J. Zhou, X. Jiao, M. Han, X. Zhang, H. Hu, R. Su, Y. Zhang, *ACS Nano* **2024**, *18*, 10324–10340.

[4] H. Asokan-Sheeja, S. Yang, A. A. Adones, W. Chen, B. B. Fulton, U. K. Chintapula, K. T. Nguyen, C. J. Lovely, C. A. Brautigam, K. Nam, *Chem. Asian J.* **2022**, *17*, e202200724.

[5] a) H. Dong, S. E. Paramonov, L. Aulisa, E. L. Bakota, J. D. Hartgerink, *J. Am. Chem. Soc.* **2007**, *129*, 12468–12472; b) H. Asokan-Sheeja, K. Awad, J. Xu, M. Le, J. N. Nguyen, N. Nguyen, T. P. Nguyen, K. T. Nguyen, Y. Hong, V. G. Varanasi, *Biomacromolecules* **2024**, *25*, 2814–2822; c) D. Xu, W. Chen, Y. J. Tobin-Miyaji, C. R. Sturge, S. Yang, B. Elmore, A. Singh, C. Pybus, D. E. Greenberg, T. J. Sellati, *ACS Infect. Dis.* **2018**, *4*, 1327–1335.

[6] a) M. Biancalana, S. Koide, *Biochimica et Biophysica Acta (BBA)-Proteins Proteomics* **2010**, *1804*, 1405–1412; b) S. Namioka, N. Yoshida, H. Konno, K. Makabe, *Biochemistry* **2020**, *59*, 2782–2787.

Manuscript received: August 15, 2024
Accepted manuscript online: October 10, 2024
Version of record online: November 13, 2024